



ORIGINAL ARTICLE

Tissue-specific models of spinal muscular atrophy confirm a critical role of SMN in motor neurons from embryonic to adult stages

Angela S. Laird^{1,2,†}, Nikolce Mackovski¹, Silke Rinkwitz³, Thomas S. Becker³ and Jean Giacomotto^{3,4,†,*}

¹ANZAC Research Institute, Concord Repatriation Hospital, University of Sydney, Sydney, New South Wales, Australia, ²Department of Biomedical Sciences, Faculty of Medicine & Health Sciences, Macquarie University, Sydney, Australia, ³Brain and Mind Research Institute, Sydney Medical School, University of Sydney, Camperdown, New South Wales 2050, Australia and ⁴Queensland Brain Institute, The University of Queensland, Building #79, St Lucia, Queensland 4072, Australia

*To whom correspondence should be addressed. Tel: +61 4 2307 1651; Email: giacomottojean@gmail.com; j.giacomotto@uq.edu.au

Abstract

Spinal muscular atrophy (SMA) is an autosomal recessive disease linked to survival motor neuron (SMN) protein deficiency. While SMN protein is expressed ubiquitously, its deficiency triggers tissue-specific hallmarks, including motor neuron death and muscle atrophy, leading to impaired motor functions and premature death. Here, using stable miR-mediated knockdown technology in zebrafish, we developed the first vertebrate system allowing transgenic spatio-temporal control of the *smn1* gene. Using this new model it is now possible to investigate normal and pathogenic SMN function(s) in specific cell types, independently or in synergy with other cell populations. We took advantage of this new system to first test the effect of motor neuron or muscle-specific *smn1* silencing. Anti-*smn1* miRNA expression in motor neurons, but not in muscles, reproduced SMA hallmarks, including abnormal motor neuron development, poor motor function and premature death. Interestingly, *smn1* knockdown in motor neurons also induced severe late-onset phenotypes including scoliosis-like body deformities, weight loss, muscle atrophy and, seen for the first time in zebrafish, reduction in the number of motor neurons, indicating motor neuron degeneration. Taken together, we have developed a new transgenic system allowing spatio-temporal control of *smn1* expression in zebrafish, and using this model, we have demonstrated that *smn1* silencing in motor neurons alone is sufficient to reproduce SMA hallmarks in zebrafish. It is noteworthy that this research is going beyond SMA as this versatile gene-silencing transgenic system can be used to knockdown any genes of interest, filling the gap in the zebrafish genetic toolbox and opening new avenues to study gene functions in this organism.

Introduction

Spinal muscular atrophy (SMA) is an autosomal recessive human disease characterized by progressive muscle weakness, motor neuron loss and premature death (1). SMA is a leading genetic cause of infant death. SMA is caused by low levels (not complete

absence) of survival motor neuron (SMN) protein, a ubiquitously expressed protein involved in multiple cellular mechanisms including RNA splicing and metabolism (2,3). The SMN protein is encoded by a gene highly conserved across different species, and complete loss-of-function is lethal in all organisms tested so far. In humans, there are two nearly identical genes encoding

[†]A.S.L. and J.G. are co-first authors.

Received: December 10, 2015. Revised: February 9, 2016. Accepted: February 15, 2016

© The Author 2016. Published by Oxford University Press. All rights reserved. For Permissions, please email: journals.permissions@oup.com

the SMN protein, SMN1 and SMN2 (1,3,4). SMN2 contains a mutation that leads to its inefficient splicing and to an unstable truncated protein (for review see 3,4). Additionally, SMN2 is present in multiple copies, with variable numbers between individuals. All SMA patients present full SMN1 loss-of-function that is partially rescued by SMN2 activity and copy numbers. Four types of SMA have been described, from severe to mild, which are directly correlated to the amount of residual functional SMN protein present.

SMA is poorly understood to date. One important question that remains unsolved is why ubiquitous low levels of SMN affects specifically the neuromuscular system despite its function being critical for the viability of all cells? It is also unclear if increasing SMN levels in motor neurons alone would be sufficient to improve the condition of SMA patients, or if high levels of this protein are also required in muscles and/or other cell types (5). This information is important for the development of future treatments aiming to compensate for the loss of SMN function. Several studies, conducted on different organisms, have tried to tackle these difficult questions, but as presented later, the findings are varied. Both muscle and neuronal knockout of *smn1* are lethal in mice and in all organisms tested so far (6,7). While Nicole et al. have shown that partial restoration of SMN levels in muscle satellite cells markedly improves phenotypes in SMA mice, a later study by Gavrilina et al. found that muscle-specific expression of SMN has no phenotypic effect (6,8). It has also been demonstrated that pan-neuronal expression of SMN ameliorates phenotypes and improves the survival of different SMA mouse models, but is not sufficient to restore wild-type conditions (8,9). Studies conducted in *Drosophila* indicate an important role of muscular expression of SMN in the progression of the disease (10,11), while others suggest a prominent role of neuronal SMN (12–14). In zebrafish, it has been shown that transient ubiquitous *smn1* knockdown, using morpholino, leads to developmental defects, including motor neuron abnormalities (15). A complete loss-of-function mutant line has further been described, and expression of human SMN specifically in motor neurons only slightly improves neuromuscular defects and survival of these knockout fish (16,17). While this modest effect suggests that motor neurons are not the only cells involved in the progression of the disease, caution has to be taken as the beneficial role of motor neuron-expressed SMN may have been underestimated. Indeed, the *smn1*-mutant zebrafish have a complete absence of SMN in all other tissues, rather than just the partial loss-of-function found in SMA patients. Taken together, these findings show that SMN is a critical protein, and more evidence is required to conclude on its tissue-specific toxicity and function.

Using a newly developed heritable gene-silencing approach (i.e. miRNA-mediated knockdown), we recently recapitulated for the first time in zebrafish the different forms of SMA (18). In practice, a transgene that ubiquitously expresses a fluorescent marker [discosoma red fluorescent protein (dsRED)] and a synthetic miRNA directed against the *smn1* gene were integrated into the zebrafish genome, resulting in ubiquitous and stable down-regulation of *smn1* gene expression. Transgenic animals developed motor neuron malformations, abnormal motor functions, scoliosis-like body deformities and premature death, with severity and age of onset directly correlated to the level of *smn1* gene inhibition, thus mimicking hallmarks observed in patients. These models are of high value to interrogate the disease. For example, the line mimicking the severe form of SMA allows the generation of larvae that present poor motor functions starting from 4 dpf (days-post-fertilization), thereby offering the unique opportunity to set up simple screening assays for both chemical and genetic experiments (19–21). Alternatively, mild models of the disease allow investigation of late-onset/adult phenotypes.

Here, we used this transgenic gene-silencing approach to establish in zebrafish the first inducible system allowing tissue-specific control of *smn1* gene expression. This system offers the ability to inhibit SMN function in any cell type of the zebrafish, independently or in combination. We first focused on analysing the effect of low-level expression of SMN in motor neurons and in muscle cells. We found that expression of anti-*smn1* miRNAs in motor neurons reproduced most hallmarks observed previously in the ubiquitous knockdown model (18). In contrast, expression of anti-*smn1* miRNAs in muscle did not induce strong defects. We also found that *smn1* knockdown in zebrafish motor neurons is sufficient to induce late-onset phenotype such as muscle atrophy, scoliosis-like body deformities and, seen for the first time in zebrafish, reduction in the number of motor neurons, indicating motor neuron degeneration.

Results

Design of an inducible system to control *smn1* expression spatio-temporally

In order to generate a zebrafish system allowing spatio-temporal control of *smn1* gene expression, we designed a genetic system based on *smn1* gene-silencing under the control of inducible Gal4/upstream activator sequence (UAS) technology (22) (Fig. 1). We first generated driver constructs expressing Gal4 specifically in motor neurons (HB9:Gal4) (23) or in muscles (503UNC:Gal4) (24) that we integrated independently into a transgenic marker line expressing green fluorescent protein (GFP) in motor neurons (MN:GFP), previously named (hsa-miR218-2:GFP) (25) (Fig. 1A). To select fish with integrated constructs (founders), F0 adults were outcrossed with a marker line carrying a stable copy of the UAS:mCherry construct. The best founders for each driver construct were selected on the basis of brightness of mCherry-fluorescence. These founders were then outcrossed with MN:GFP to generate stable F1 HB9:Gal4;MN:GFP and 503UNC:Gal4;MN:GFP lines.

For the responder construct, we took advantage of our previous work in which we demonstrated the efficiency of two synthetic anti-*smn1* miRNAs to trigger *smn1* knockdown; these synthetic miRNAs were named miRsmn1-1 and miRsmn1-4 (Fig. 1B and C) (18). Independently, both of these synthetic miRNAs were able to trigger stable and potent *smn1* gene-silencing and recapitulate SMA hallmarks in zebrafish (18). In order to increase the potency of this *smn1* gene-silencing system, we concatenated four anti-*smn1* miRNAs with two copies of both miRsmn1-1 and miRsmn1-4 (Fig. 1B). These sequences were fused to dsRED and cloned under the control of the UAS promoter. This gene-silencing responder construct was integrated into the MN:GFP zebrafish line. F0 fish were outcrossed with previously selected F1 503UNC:Gal4;MN:GFP in order to identify founders (dsRED expression in muscles is easy to detect). Several founders were identified, and one (UAS:miRsmn1-4141#100) was selected for its strong and homogeneous dsRED expression. We outcrossed this UAS:miRsmn1-4141#100 founder with both 503UNC:Gal4;MN:GFP and HB9:Gal4;MN:GFP to produce HB9:Gal4;UAS:miRsmn1-4141#100;MN:GFP (henceforth called HB9:Gal4;UAS:miRsmn1) and 503UNC:Gal4;UAS:miRsmn1-4141#100;MN:GFP (called 503UNC:Gal4;UAS:miRsmn1) fish. Thirty positive F1 embryos presenting homogeneous dsRED expression in muscle or in motor neurons were selected and raised to adult stage. It is noteworthy that it was difficult to obtain large numbers of HB9:Gal4;UAS:miRsmn1 adults due to a high death rate (see later), suggesting that zebrafish are particularly

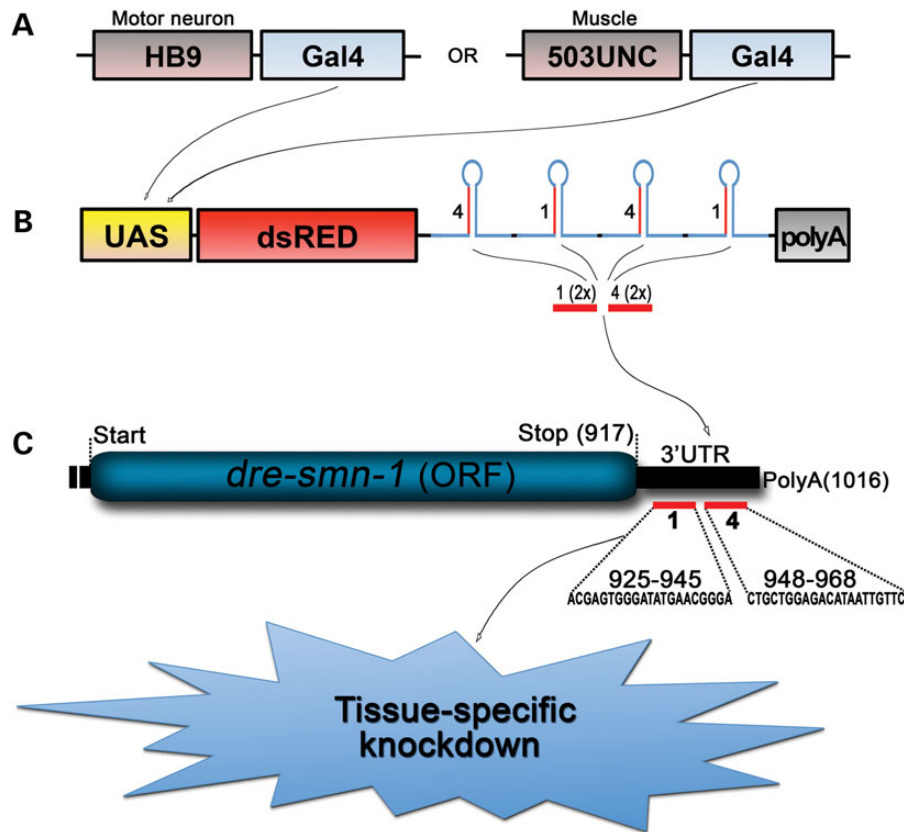


Figure 1. Inducible *smn1* miRNA-mediated knockdown system. In order to down-regulate *smn1* tissue specifically, we established an inducible transgenic system based on Gal4/UAS technology. (A) Driver constructs expressing Gal4 in muscle cells (503UNC promoter) or in motor neurons (HB9 promoter). (B) Responder construct that, in the presence of Gal4, expresses a transcript containing mCherry sequence followed by four artificial *pri-miRs*. (C) The *pri-miRs* were designed to release anti-*smn1* miRNAs that bind to two confirmed target sites of *dre-smn1*.

sensitive to *smn1* silencing in motor neurons. Additionally, we found it difficult to generate a line expressing high levels of dsRED:miRsmn1 in motor neurons. HB9:Gal4;UAS:miRsmn1, presented here, which is the brightest of all motoneuron *smn1* knock-down lines generated, presents weak dsRED fluorescence intensity (reflecting synthetic anti-*smn1* miRNA expression) compared with control or 503UNC:Gal4;UAS:miRsmn1 (Supplementary Material, Fig. S1). The difficulty in obtaining a high-expression line when the HB9 driver was used supports the hypothesis that *smn1* silencing is particularly toxic in motor neurons.

As a control, we introduced a construct containing 4× control-miRs fused to dsRED under the control of an ubiquitous promoter into MN:GFP embryos, as described earlier.

Motor neuron but not muscle *smn1* knockdown recapitulates SMA hallmarks

We showed previously that ubiquitous *smn1* knockdown led to a strong larval phenotype, including abnormalities in motor neuron development, shorter body size, premature death and abnormal swimming behaviour (18). In order to test whether such phenotypes could be reproduced by inhibiting *smn1* tissue specifically, F1 controls, HB9:Gal4;UAS:miRsmn1 and 503UNC:Gal4;UAS:miRsmn1 were incrossed to generate F2 embryos. Twenty embryos per condition were selected on the basis of homogeneous dsRED expression and used for further analysis. We first took advantage of GFP expression induced by the MN:GFP transgene in order to evaluate primary motor neuron development *in vivo* (Fig. 2A). There are four types of primary motor neurons,

including Caudal Primary (CaP) motor neurons that project long axons ventrally (26). We focused on the CaP motor neurons and quantified projection abnormalities at 30 and 52 hpf (hour-post-fertilization). Motoneuronal *smn1* inhibition reproduced similar abnormalities to those observed previously following ubiquitous gene-silencing, including short axons, abnormal branching and pathfinding errors (Figs. 2A and 3). At 52 hpf, F2 HB9:Gal4;UAS:miRsmn1 fish presented 1.6(±0.3) abnormal CaP motor neuron projections per side compared with 0.3(±0.1) in control. It is noteworthy that the extent of these defects was relatively modest compared with defects observed previously with ubiquitous *smn1* knockdown, wherein approximately three abnormal CaP projections were observed per side of fish at 52 hpf (18). Fish expressing anti-*smn1* miRNAs in muscles did have slightly higher numbers of abnormal motor neuron projections than controls at 30 hpf, but this difference was no longer detectable at 52 hpf (Fig. 2A). Similar results were obtained by analysing larvae immunostained for GFP or synaptic vesicle-2, confirming the *in vivo* observations (Fig. 3).

In contrast, neither motor neuron knockdown nor muscle knockdown reproduced the significant reduction of body length observed in the ubiquitous *smn1* knockdown model (Fig. 2B) (18).

We then analysed larval swimming behaviour and found that motor neuron knockdown, but not muscle knockdown, reduced motor function of zebrafish (Fig. 2C). This difference was detectable from 5 dpf with increased impairment developing with age, similar to results obtained previously with ubiquitous *smn1* gene inhibition (18).

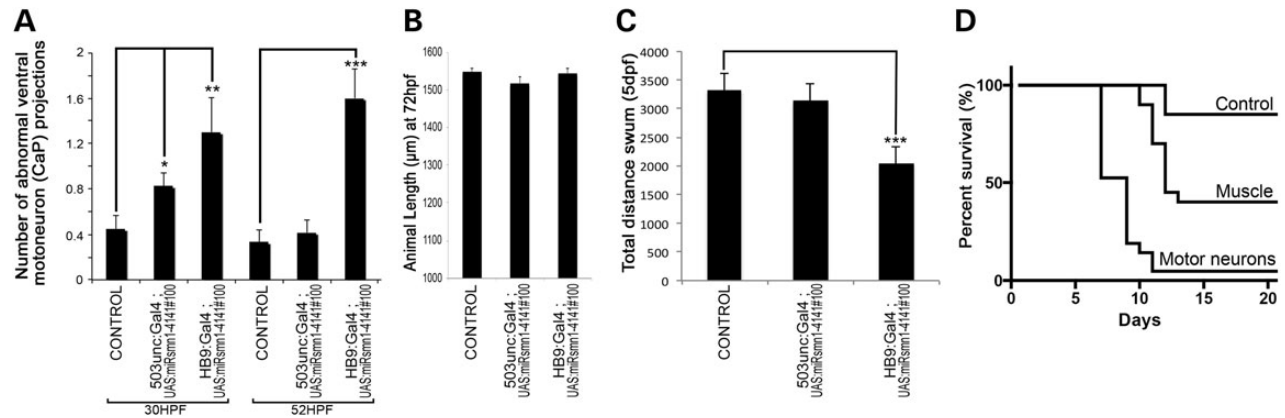


Figure 2. Phenotypes induced by muscle- and motor neuron-specific *smn1* knockdown. (A) Number of ventral motoneuron (CaP) abnormalities (short axons, abnormal branching, pathfinding errors and/or absence of cell body) observed per side of control animals and larvae expressing anti-*smn1* miRs in muscle (503UNC:Gal4;UAS:miRsmn1) or in motor neurons (HB9:Gal4;UAS:miRsmn1), at 30 and 52 hpf. (B) Animal size comparison between control animals and larvae expressing anti-*smn1* miRs specifically in muscle or motor neurons. (C) Average distance (arbitrary unit) swum by 5 dpf larvae over 16 min. (D) Survival assay comparing control and tissue-specific *smn1* knockdown animals (F2 lines, 20 larvae per group). (A and B) Means of 20 larvae \pm standard error of the mean. (C) Mean of 12 larvae \pm standard error of the mean. Different from control at * $P < 0.04$, ** 0.02 , and *** 0.001 .

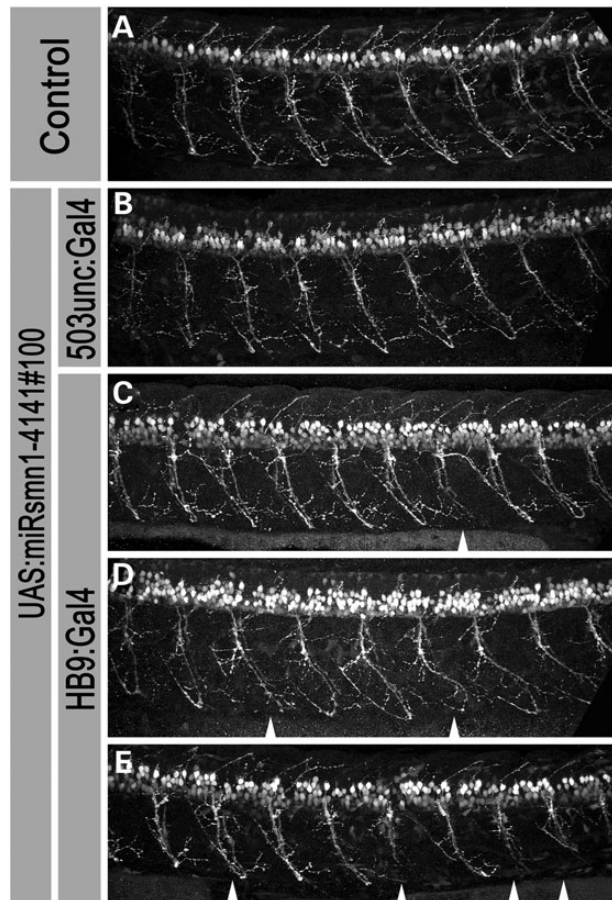


Figure 3. Representative images of 52 hpf zebrafish larvae expressing GFP in motoneurons \pm tissue-specific *smn1* knockdown (anti-GFP immunostaining). Lateral views of (A) control and (B–E) transgenic zebrafish larvae expressing artificial miRs (targeting *smn1* 3'UTR) specifically in muscle cells (B) or in motor neurons (C–E). Compared with control and 503UNC:Gal4;UAS:miRsmn1 animals, larvae expressing anti-*smn1* miRs in motor neurons HB9:Gal4;UAS:miRsmn1 showed abnormal motor neuron development including abnormal branching, short axons and pathfinding errors (white arrowheads).

Finally, we found that both motor neuron and muscle gene inhibition induced premature zebrafish death, but with dramatic effects for motor neuron knockdown (Fig. 2D). In the first 11 days of life, 95% of F2 HB9:Gal4;UAS:miRsmn1 animals died, and no fish survived until adulthood (as observed previously) (18). Considering the absence of motoneuronal and motor phenotype in F2 503UNC:Gal4;UAS:miRsmn1, it was, however, surprising to see that 60% of those larvae died in the first 13 days. In contrast to motoneuronal knockdown, all fish that survived this critical period did reach adulthood. They did not present any sort of detectable phenotype at adult stages. After a closer investigation of the developing 503UNC:Gal4;UAS:miRsmn1 larvae, we found that all the fish that died in the 13 dpf period were not able to inflate their swim bladder. No other phenotype was observed in these larvae.

Human SMN1 mRNA rescues motor neuron *smn1* knockdown phenotypes

To validate the specificity of *smn1* knockdown in the experiments presented earlier, we injected human SMN1 mRNA into F2 embryos. We showed previously that 200–400 pg of human SMN1 mRNA was enough to partially rescue motor neuron phenotype induced by ubiquitous *smn1* knockdown (18). Here, injection of human SMN1 RNA (250 pg) did not lead to any obvious defect in F2 control or F2 503UNC:Gal4;UAS:miRsmn1 larvae, but significantly reduced motor neuron abnormalities present in F2 HB9:Gal4;UAS:miRsmn1 animals at 52 hpf (Fig. 4). However, *hsa*-SMN1 RNA did not delay premature death observed in either motor neuron- or muscle-specific *smn1* knockdown.

Motor neuron *smn1* knockdown induces late adult phenotypes

As described earlier, F2 HB9:Gal4;UAS:miRsmn1 developed severe early defects leading to impaired motor function and decreased survival. Additionally, we observed late-onset abnormalities in the F1 fish. First, compared with control and F1 503UNC:Gal4;UAS:miRsmn1, fish expressing anti-*smn1* miRNAs in motor neurons presented a high death ratio (Supplementary Material, Fig. S2). Only 7/30 HB9:Gal4;UAS:miRsmn1 fish reached adulthood, while 24/30 and 21/30 survived in control and muscle knockdown

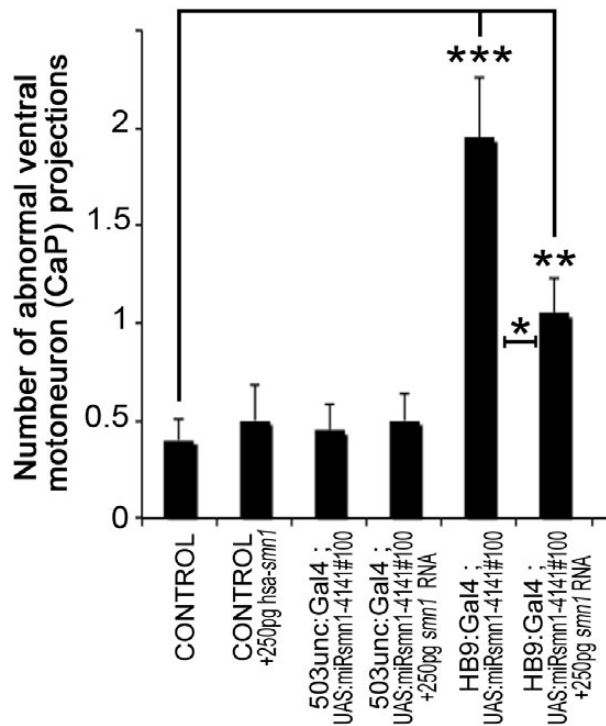


Figure 4. SMN1 mRNA rescues CaP projection abnormalities observed in larvae presenting motor neuron-specific *smn1* knockdown. Injection of 250 pg of hsa-SMN1 RNA reduces motor neuron phenotypes observed in 52 hpf (HB9:Gal4; UAS:miRsmn1) larvae. Means of 20 larvae \pm standard error of the mean. Significant difference at * $P < 0.02$, ** 0.01 , and *** 0.0001 .

groups, respectively. While these seven fish had only slightly shorter body lengths compared with the other groups, they presented with strong weight loss at adult stages (96 dpf) (Fig. 5A–C). All seven HB9:Gal4;UAS:miRsmn1 fish presented with an obviously thin trunk, suggesting muscle atrophy (Fig. 5D). They also presented with severe body deformities (scoliosis-like phenotype) and abnormal swimming behaviour/coordination, phenotypes that were developing progressively (Fig. 5D–F; Supplementary Material, Video S1). Scoliosis is a typical hallmark of mild forms of SMA and progresses with age, as observed in our model (27,28). These deformities were correlated to muscle atrophy and poor strength/structural balance in SMA patients. Prior to sacrificing these animals to ascertain muscle atrophy, we analysed their motor function. While no difference was detected between control and muscle knockdown, motor neuron *smn1* knockdown significantly reduced overall distance swum and swimming speed, suggesting poor muscle strength (Fig. 6A–E). These fish presented not only with severely impaired motor function but also with loss of coordination, suggesting muscular imbalance and/or abnormal muscular control (Supplementary Material, Video S1).

To check the specificity of the results presented earlier, we crossed a previously generated and validated transgenic line expressing ubiquitously human SMN1 (18) with F1 HB9:Gal4;UAS:miRsmn1 and F1 control fish. No obvious defects were detected in the resultant F2 fish, confirming the specificity of the results presented earlier.

Motor neuron *smn1* knockdown induced muscle atrophy and motor neuron cell death

We sacrificed and fixed adult F1 fish (4 months old) to examine their morphology. It is noteworthy that at the time of these

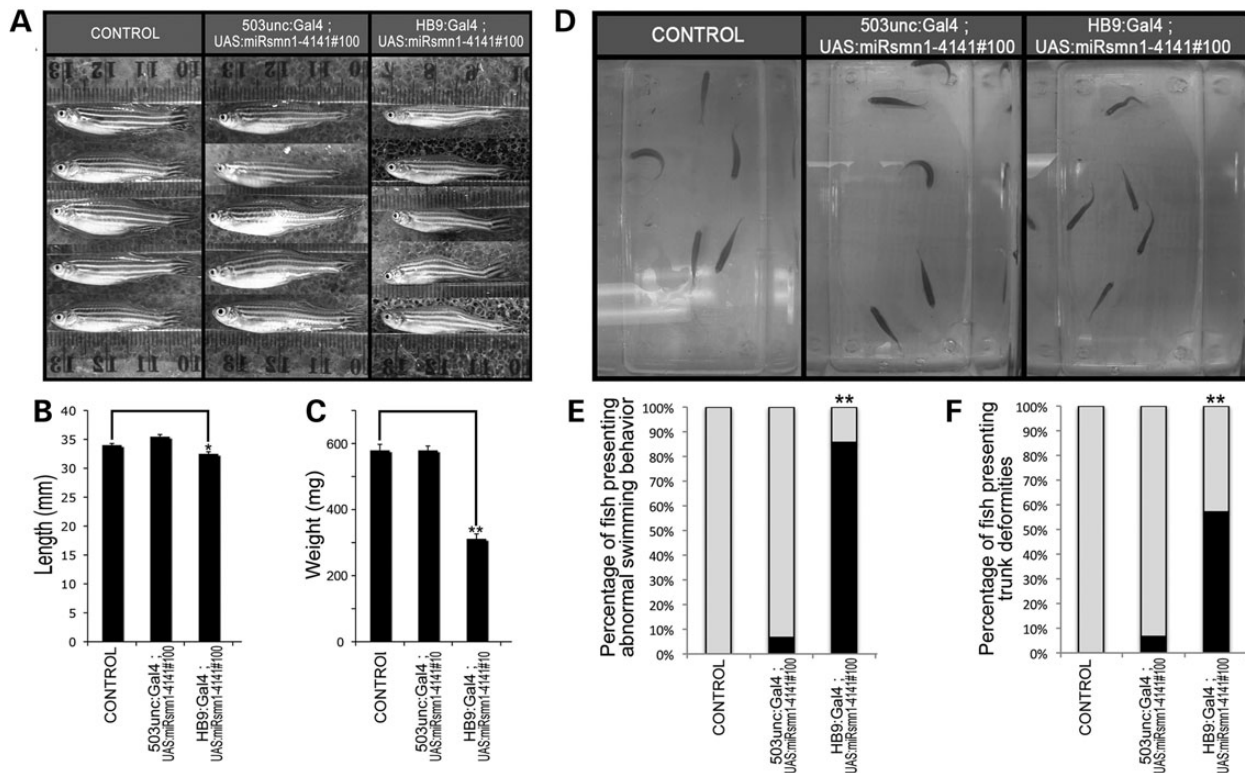


Figure 5. Motor neuron *smn1* knockdown induces adult phenotypes. Motor neuron *smn1* knockdown induces adult phenotypes including a slightly shorter body length (A and B), marked body weight loss (C), abnormal swimming behaviour and coordination (D and E) and marked trunk deformities (scoliosis-like) (D and F). Figure shows 96 dpf animals, with $n = 15$ [8 females (F)/7 males (M)] for control, $n = 15$ (9F/6M) for 503unc:Gal4;UAS:miRsmn1 and $n = 7$ (3F/4M) for HB9:Gal4;UAS:miRsmn1. B and C present means \pm standard error of the mean. Different from control at * $P < 0.05$ and ** 0.001 .

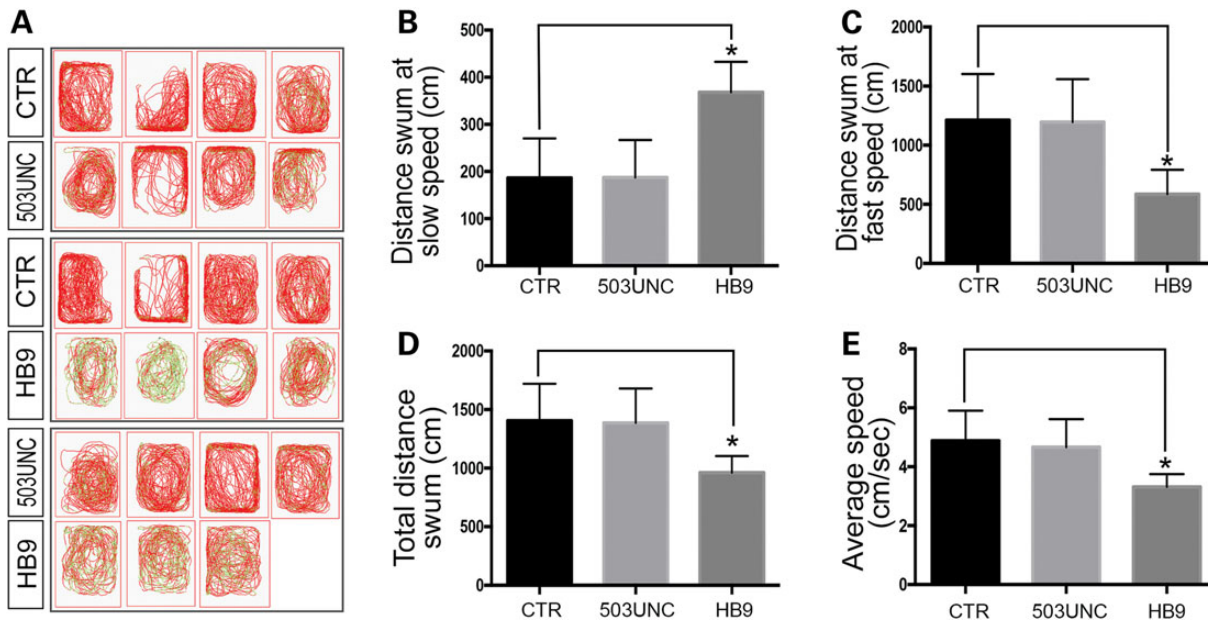


Figure 6. Analysis of spontaneous swimming behaviour of adult (96 dpf) zebrafish. (A) Images representing swimming tracks of adult fish during a 5 min swimming period, with green and red tracks corresponding to slow (1–3 cm/s) and high speed (>3 cm/s) movements, respectively. (B) Distance swum at slow speed during a 5 min test. (C) Distance swum at high speed during a 5 min test. (D) Total distance swum during 5 min test. (E) Average speed of animals analysed (cm/s). Means of 15 animals for CTR (control), 15 animals for F1 503UNC (503UNC:Gal4;UAS:miRsmn1) and 7 animals for F1 HB9 (HB9:Gal4;UAS:miRsmn1), \pm standard deviation (SD). Different from CTR and 503UNC at * $P < 0.00001$.

histological analysis, only four fish remained alive in the HB9:Gal4;UAS:miRsmn1 group (Supplementary Material, Fig. S2). We cut transverse sections of the whole zebrafish body in two parallel series. One series was cover-slipped immediately to allow microscopic examination of muscle cells, and the other series was mounted onto slides for cresyl violet staining. To remove variability due to regional differences in body size and motor neuron numbers, we focused on the tail region of the fish. We first measured tail width as well as muscle cells size and number by examining the non-stained series (Fig. 7). F1 503UNC:Gal4;UAS:miRsmn1 fish, presenting muscle anti-*smn1* expression, had similar tail widths to control fish, with 4.6 ± 0.18 and 4.4 ± 0.18 mm, respectively, (Fig. 7G). However, F1 HB9:Gal4;UAS:miRsmn1, presenting obviously thinner trunks (Fig. 5; Supplementary Material, Video S1), had significantly smaller tail widths, 3.0 ± 0.2 versus 4.4 ± 0.18 mm for the control (Fig. 7G). Analysis of muscle cell sizes confirmed that HB9:Gal4;UAS:miRsmn1 fish had atrophic muscle fibres compared with controls (770 ± 139 versus $1315 \pm 111 \mu\text{m}^2$, respectively) (Fig. 7H). HB9:Gal4;UAS:miRsmn1 presented also with fewer muscle cells than control, with an average of 99.2 ± 56 versus 219.4 ± 26 cells per section, respectively, (Fig. 7I). The average size and number of muscle cells in 503UNC:Gal4;UAS:miRsmn1 fish were not significantly different from controls; 1326 ± 108 versus $1315 \pm 107 \mu\text{m}^2$, respectively, for muscle fibre sizes, with 203 ± 32 and 219 ± 32 cells per section (Fig. 7H and I).

Finally, we investigated whether motor neuron death was occurring in these fish as demonstrated in SMA patients. We performed manual blinded counting of large motor neurons in the cresyl-violet-stained sections (Fig. 7J–M). We did not observe any significant differences in the number of motor neurons between 503UNC:Gal4;UAS:miRsmn1 and control fish, with an average of 22.2 ± 2.7 and 23.4 ± 3.7 motor neurons per region, respectively (Fig. 7J). However, HB9:Gal4;UAS:miRsmn1 fish presented significantly fewer motor neurons than controls, with

an average of 11.0 ± 3.3 versus 23.4 ± 3.7 motor neurons in the control group (Fig. 7J). This result strongly suggests that motor neuron degeneration takes place in zebrafish following silencing of the *smn1* gene, and that specific motoneuronal silencing is enough to induce this degenerative phenotype. It is noteworthy that these results might be under-evaluated as the four adult HB9:Gal4;UAS:miRsmn1 fish euthanized for the histological processing were the only fish that survived to 4 months of age, and likely the least affected fish in the group (Supplementary Material, Fig. S2).

Discussion

We have developed, and validated in zebrafish, a new transgenic system based on miRNA-mediated knockdown allowing manipulation of SMN protein function spatio-temporally in an inducible manner. This new system will complement existing models in order to study SMN protein function. It offers the opportunity to investigate the role of diverse cell types, independently or in synergy, in SMA phenotypes and progression. This system also offers the possibility to control SMN function temporally, thus helping to respond to questions related to the timing of SMN restoration in regards to potential therapeutic treatments. In this study, we first used this transgenic system to test independently the effect of a low level of SMN protein in motor neurons and in muscles in regards to SMA phenotypes and progression.

We found that motor neurons are particularly sensitive to *smn1* knockdown. Expression of anti-*smn1* miRNAs in motor neurons alone reproduced most hallmarks observed in our previous SMA model based on ubiquitous *smn1* knockdown (18). Indeed, reduction of SMN function in motor neurons was enough to reproduce defects in motor neuron development, poor motor function and premature death of zebrafish embryos and larvae, suggesting that low levels of SMN protein in motor neurons are sufficient to trigger SMA in zebrafish. Additionally, motor

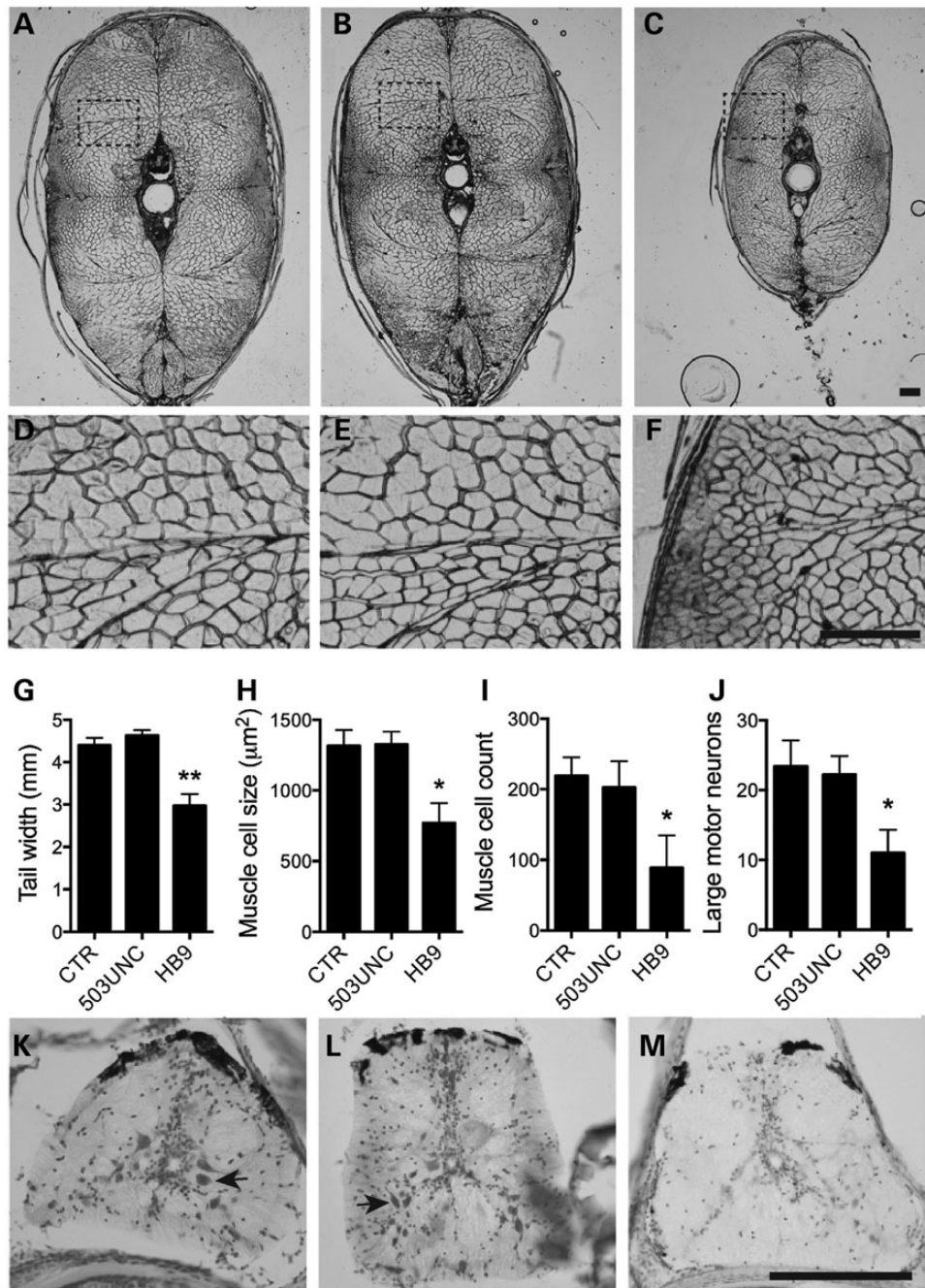


Figure 7. Motor neuron *smn1* knockdown leads to motor neuron degeneration and muscle atrophy. (A–C) Transverse sections through whole adult (4-month-old) zebrafish bodies revealed that control (A) and 503UNC-Gal4;UAS:miRsmn1 (B) fish have larger body widths than HB9-Gal4;UAS:miRsmn1 (C) zebrafish. (D–F) Higher magnification of the indicated area (dashed box) provides a view of the number and size of muscle cells of Control (D), 503UNC-Gal4;UAS:miRsmn1 (E) and HB9-Gal4;UAS:miRsmn1 (F) fish. Quantification of the average tail width (G) for each fish revealed that HB9-Gal4;UAS:miRsmn1 have far narrower tails than control (CTR) and 503UNC-Gal4;UAS:miRsmn1. HB9-Gal4;UAS:miRsmn1 also had smaller muscle cell size (H) and muscle cell count (I). (J–M) Cresyl violet staining of transverse sectioned whole zebrafish allowed visualization of motor neurons within the zebrafish spinal cord. Blinded counting of motor neurons was performed on sections from control (K), 503UNC-Gal4;UAS:miRsmn1 (L) and HB9-Gal4;UAS:miRsmn1 (M) zebrafish. Examples of large motor neurons are indicated with an arrow. (J) Comparison of the total number of motor neurons within a tail region (eight sections) revealed that HB9-Gal4;UAS:miRsmn1 fish have fewer motor neurons than controls. All scale bars indicate 200 μm . Graphed values indicate mean \pm standard error mean. Significantly different from control at * $P < 0.05$ and ** 0.003 .

neuron-specific *smn1* knockdown reproduced late-onset defects, including weight loss, muscle atrophy, abnormal motor function and scoliosis similar to that observed in our previous zebrafish model and in patients (18,27). Microscopic anatomical analysis also revealed that HB9-Gal4;UAS:miRsmn1 animals had a reduced number of motor neurons, indicating motor

neuron degeneration. We hypothesize that this motor neuron loss is the cause of muscle atrophy and, subsequently, of progressive body deformities and abnormal motor function in the motor neuron *smn1* knockdown fish. Use of our model would be useful to confirm and investigate the timing of such events in the future. It would also be interesting to analyse the timing and progression

of such phenotypes, and see if restoration of SMN later in life is sufficient to restore normal muscle mass and/or overall normal behaviour and lifespan.

It is noteworthy that, while motor neuron *smn1* knockdown reproduced most hallmarks of SMA in zebrafish, we observed that motor neuron projection defects at 30 and 52 hpf were relatively modest when compared with defects observed in the previously described ubiquitous knockdown model (Fig. 2A) (18). Several hypotheses could explain this difference. First, the HB9 promoter used to drive expression of the anti-*smn1* miRNAs initiates expression in differentiated motor neurons, whereas the previously used ubiquitous Ubiquitin promoter initiates expression at an earlier stage. This means that in the present study, motor neurons would contain SMN protein at the beginning of their life while the motor neurons of fish with ubiquitous knockdown were already loaded with synthetic miRNAs, and thereby already depleted of SMN protein. Second, additional cells, other than motor neurons, may play a role in this developmental phenotype. Results from a recent study support this hypothesis, suggesting that neuronal networks upstream of motor neurons are most likely involved in SMA hallmarks (12). Considering the versatility of our new knockdown approach, it would be interesting to test the role of SMN in these upstream circuits, in synergy with or independently of motor neurons, in regards to this early motor neuron phenotype.

Additionally, our study suggests that muscles are relatively resistant to *smn1* knockdown from embryonic to adult stages. However, and for a reason that we cannot conceptualize, reduction of SMN protein in muscles seems to strongly affect swim bladder function in zebrafish, subsequently leading to premature death. No other abnormalities were detected in zebrafish with muscle-specific expression of anti-*smn1* miRNAs.

The transgenic system presented here opens new avenues to manipulate SMN in zebrafish, and thus to study SMA. However, it has some limitations. First, it is difficult to reproduce with accuracy the same level of knockdown in the different tissues of the fish. For instance, by considering dsRED fluorescence intensity, reflecting anti-*smn1* miRNAs expression and thereby knockdown potency, it is likely that HB9:Gal4;UAS:miRsmn1 presents a much lower level of *smn1* silencing than 503UNC:Gal4;UAS:miRsmn1. Unfortunately, while we showed previously that the observed fluorescence intensity can be used to qualitatively evaluate knockdown level (18), it is difficult to quantify this inhibition efficiently in such restricted tissues. We tried to isolate motor neurons and muscle cells in order to quantify the level of *smn1* inhibition in our line, but we were unable to develop a method robust enough to get reliable results. The use of a cell sorter might allow accurate quantification of the level of *smn1* knockdown. This would allow us to evaluate the threshold concentration of SMN protein that is required in zebrafish motor neurons to either trigger SMA hallmarks or maintain normal functions. Another important limitation of our model is the Gal4/UAS system *per se*. The UAS sequence contains CpG islands that attract methylation, which makes it prone to silencing (29). Such events occur randomly and are difficult to control. Luckily, fluorescent expression can be used to manually collect the appropriate embryos to raise and study. However, this approach requires practice, is time consuming and is not compatible with large-scale experiments. An option would be to use the CRE/Lox system (30) instead of Gal4/UAS. The knockdown cassette would be kept silent and activated (by sequence deletion or inversion) in the desired cells. This would in theory improve homogeneity and ease of the experiments. Nevertheless, the current model is useful for studying the

pathogenic mechanisms of SMA and performing low-throughput studies.

Taken together, we have developed the first zebrafish model of SMA that allows investigation of the spatio-temporal effects of SMN protein level on SMA development. We have also used this model to study the role of specific cell types in the development and progression of SMA. Knockdown of *smn1* in motor neurons alone was sufficient to produce not only early phenotypes of SMA such as motor neuron abnormalities, larval motor dysfunction and decreased survival, but also late-stage hallmarks such as muscle atrophy, scoliosis-like body deformities, motor dysfunction and reduction of motor neuron number. Further studies, harnessing the ability of this model to produce spatio-temporal control of *smn1* gene expression would provide further insight into normal and pathogenic SMN function(s). Last but not least, while we focused on *smn1*, the transgenic gene-silencing system presented here goes beyond SMN function(s) and SMA as this knockdown technology is applicable to any gene of interest, opening a new avenue to study gene function(s) and mimicking human diseases in zebrafish.

Materials and Methods

Zebrafish maintenance and transgenic lines

Adult zebrafish and embryos were maintained and studied using protocols approved by the University of Sydney and the University of Queensland Animal Ethics Committees.

Generation of HB9:Gal4 and 503UNC:Gal4 plasmids

To generate the driver construct expressing Gal4 in motor neurons, HB9:Gal4, we first produced an intermediate p5E-HB9 to12 kit-compatible clone. The HB9 promoter (3.3 kb) was extracted by digestion (*EcoRI* and *BamHI*) from a plasmid kindly provided by Dirk Meyer (23) and cloned into p5E-MCS(228). p5E-HB9 was then combined with pME-Gal4VP16(387) and p3E-polyA(302) in the destination clone pDestTol2pA2(394) to generate the final HB9:Gal4 plasmid used in this study.

To construct the driver construct expressing Gal4 in muscles, we started with p5E-503UNC, previously published (24), and combined it in the same way described for HB9:Gal4 generation. The final plasmid was named 503UNC:Gal4.

Generation of anti-*smn1* miRNAs

The anti-*smn1* miRNA, miRsmn1-1 and miRsmn1-4, were designed, cloned and validated previously (18). Both synthetic miRNAs were cloned into pME-RNAi652 that contains dsRED and that is compatible with the tol2kit (31).

Generation of UAS:dsRED:smn1-4141 plasmid and control

In order to construct a UAS:dsRED:smn1-4141 presenting 4× repeat of anti-*smn1* synthetic miRNA, with two copies of miRsmn1-1 and of miRsmn1-4, we first generated a pME-dsRED:smn1-4141 vector. We digested dsRED-containing pME-RNAi652-miRsmn1-1 with *BamHI* and *XhoI* and extracted by gel purification the cassette containing miRsmn1-1 (Supplementary Material, Fig. S3). MiRsmn1-1 was then fused in 3' of miRsmn1-4 in purified pME-RNAi652-miRsmn1-4 digested by *BglII* and *XhoI*. The resulting plasmid contains a 2× repeat of synthetic miRNA and was named pME-RNAi652-miRsmn1-41. The same procedure was repeated to extract the miRsmn1-41 sequence

and to fuse it into pME-RNAi652-miRsmn1-41, thus generating pME-RNAi652-miRsmn1-4141. pME-RNAi652-miRsmn1-4141 was combined with p5E-UAS(327) into a homemade mini tol2-R4R2 (1494) destination clone. The resulting plasmid was named UAS:dsRED:smn1-4141.

To generate the control construct, we first generated pME-RNAi652-4xCTR that contains a 4× repeat of a control miRNA. The control miRNA (AAGCACAAACGCGACATGGTTA) was generated in a previous study. It was originally designed to target an artificial 3'UTR in order to validate our RNAi tools (18). This control miRNA does not recognize any mRNA in zebrafish. Control-miRs (4×) were cloned together using the same procedure as described earlier and shown in Supplementary Material, Figure S3. A final plasmid was then generated using p5E-βactin (ubiquitous promoter) and minitol2-R4R2(1494) destination clone. The resulting plasmid was named βactin:dsRED:4xCTR (abbreviated to CTR in figures).

DNA injection and transgenic line selection

To integrate DNA constructs into the zebrafish genome, 1 nl of a mix containing 30 ng/μl of DNA of interest plus 25 ng/μl of transposase mRNA and phenol red were injected at one-cell stage into MN:GFP zebrafish embryos; a transgenic line that specifically expresses GFP in motor neurons. Note that MN:GFP was previously named hsa-miR218-2:GFP in our laboratory and communications (25).

Immunohistochemistry

Whole mount immunostaining was performed to label motor axons, as described previously (32) using anti-GFP (1:1000, AMS Biotechnology cat # TP401) and anti-rabbit Alexa Fluor® 488 (A-11034) secondary antibody (33). We also performed additional immunostaining using anti-acetylated-tubulin (1:250, T7451 SIGMA) and presynaptic anti-synaptic vesicle-2 (SV2, 1:250, Developmental Studies Hybridoma Bank) with secondary antibodies anti-rabbit Alexa Fluor® 488 (A-11034, Life Technologies) and anti-mouse Alexa Fluor® 594 (A-21201, Life Technologies), respectively.

Generation of human SMN1 plasmids and RNA synthesis

Using human cDNA as template, the open reading frame and a small 3'UTR part of human SMN1 were amplified with forward primer (63-hsa-smn-atg, aattgaattcATGGCGATGAGCAGCG) and reverse primer (65-hsa-smn-reverse, ctcgagCGCTTCACATTCCA GATCTGT). The 976 bp PCR product was digested with EcoRI and XhoI and ligated in EcoRI/XhoI digested and gel purified pCS2+ vector. The corresponding plasmid was named pCS2 + hsaSMN1.

To synthesize human SMN1 RNA, pCS2 + hsaSMN1 was linearized with NotI. Sense hsa-SMN1 RNA transcription was performed using the mMESSAGING mMACHINE SP6 transcription kit (Ambion), following the manufacturer's protocol. RNA was purified using a MEGA clear kit (Ambion) following the manufacturer's protocol, aliquoted and stored at -80°C. hsa-SMN1 RNA (250 pg) was injected into the yolk of one- to four-cell-stage embryos. After injection, the remaining RNA was loaded on a gel to check for RNA degradation.

In order to generate a tol2 kit-compatible pME vector containing hsa-SMN1, pCS2 + hsaSMN1 was digested by EcoRI/BglII and the hsa-SMN1-cassette was gel purified. This cassette was cloned into an EcoRI/BamHI opened and gel purified pME-MCS(237) plasmid, and the final construct was named pME-hsaSMN1.

pME-hsaSMN1 was then combined with p5E-Ubiquitin and p3E-polyA (302) in a pDestTol2CG2(395) destination vector carrying cmlc2:GFP. The plasmid was named UBI:hsaSMN1 and used to generate transgenic lines for the rescue experiments.

Imaging

Prior to analysis, animals were embedded in 1% low-melting agarose as previously described (34). Images presented in this study were acquired using a Zeiss LSM710 confocal microscope coupled with ZEN software. Images were processed using Image J when required. For fluorescence intensity measurements, one embryo of each group was quickly scanned to define appropriate parameters, allowing signal acquisition without pixel saturation. All embryos were scanned using the same parameters. Integrated fluorescence density was evaluated on 1.05 μm stacks in Image J. The same ROI area was used for all samples. It was defined using a 'Specify ROI' plugin and consisted of an oval ROI of 19 μm².

Motor neuron phenotype quantification

In order to quantify motor neuron abnormalities, all animals were anaesthetized in tricaine and observed laterally under a fluorescent microscope, unless otherwise stated. Only CaP-axon projection abnormalities were scored. One point was tabulated for every motor axon that showed defects (abnormal branching, obvious abnormal length or absence of any projections). Scores were compared using t-tests. To validate the *in vivo* observations, immunostaining (using anti-GFP, anti-SV2 and anti-tubulin antibodies) was performed on paraformaldehyde-fixed larvae as described earlier. The same scoring system was used.

Survival assays

Adult zebrafish were pooled at the same time and mated for 1 h in order to generate synchronized embryos. Embryos were collected in E3 medium. For every condition, the 20 brightest embryos (red fluorescence) were sorted at 2 dpf and used for the survival assay. Embryos/larvae were then counted twice a day in order to record death ratio over a period of 20 days. From day 0 to day 5, animals were stored in Petri dishes, after which they were transferred into beakers containing small amounts of paramecia until day 20.

Behavioural assay (larvae)

Behaviour analyses were performed using the Zebrafish (Viewpoint) following manufacturer's instructions (<http://www.viewpoint.fr/en/p/equipment/zebrabox>). Zebrafish larvae were distributed in 24-well plates filled with E3 medium (one larvae per well). Plates were incubated at 28°C in darkness for 1 h prior to analysis. The assay involved recording larval behaviour during a 16 min protocol consisting of two repeated cycles of 4 min of light and 4 min of darkness (light-to-dark event promotes larva activity). At the end of the experiment, each larva was checked in order to exclude potential dead animals from the data. Data were exported and processed using Excel. Speed and distance swum were recorded as arbitrary units. All measurements were compared via t-tests.

Behavioural assay (adult)

The motor behaviour of 3-month-old (adult) zebrafish was examined using a ZebraTower (Viewpoint) recording device wherein

eight fish were recorded simultaneously in separate open tanks (10 cm × 12.5 cm × 6 cm deep). The test period was 5 min in ambient fluorescent light. Tracks of the swimming trajectories of the fish were recorded, and the distance swum at slow speed (1–3 cm/s) and high speed (>3 cm/s) were extracted. The total distance swum and average swimming speed were also calculated in excel. All measurements were compared via t-tests. The proportion of fish presenting with abnormal swimming behaviour and trunk abnormalities was compared using a χ^2 test.

Histological analysis

Adult (4-month-old) F1 zebrafish were sacrificed, fixed in 4% paraformaldehyde and incubated in 20% sucrose cryo-protectant solution. The whole zebrafish was mounted in OCT mounting media and snap frozen in supercooled isopentane solution prior to transverse sectioning (20 μ m) on a cryostat (−20°C). The sections from each fish were collected in two parallel series, each mounted onto separate Superfrost Plus Glass slides. One series was cover-slipped immediately to allow microscopic examination of muscle cells, and the other series was air-dried for cresyl violet histological staining. We imaged both sets of slides using a Leica DFC 500 upright microscope. A researcher blinded for experimental group used ImageJ to measure the width of each section (tail width) and performed particle analysis to detect muscle cell size and number. The cresyl violet series was also imaged, and a researcher blinded for experimental group performed manual counting of motor neurons in each section and calculated the total number of large motor neurons in the tail region (eight sections per animal). The average body width, muscle cell size, muscle cell count and motor neuron count were calculated for each fish, and t-tests were used to identify statistical differences between groups.

Supplementary Material

Supplementary Material is available at HMG online.

Authors' contributions

J.G. designed the research. J.G., A.S.L., N.M. and S.R. performed the research. J.G. and A.S.L. processed the data. A.S.L., T.B. and J.G. wrote the manuscript.

Conflict of Interest statement. None declared.

Funding

This work was funded by National Health and Medical Research Council (1024863 to S.R. and T.S.B.; and 1069235 to A.S.L., T.S.B. and J.G.). This work was also supported by grants delivered by the Rebecca L. Cooper Medical Research Foundation to J.G. and the MJD Foundation to A.S.L.

References

- Lefebvre, S., Burglen, L., Reboullet, S., Clermont, O., Burlet, P., Viollet, L., Benichou, B., Cruaud, C., Millasseau, P., Zeviani, M. et al. (1995) Identification and characterization of a spinal muscular atrophy-determining gene. *Cell*, **80**, 155–165.
- Paushkin, S., Gubitza, A.K., Massenet, S. and Dreyfuss, G. (2002) The SMN complex, an assemblyosome of ribonucleoproteins. *Curr. Opin. Cell Biol.*, **14**, 305–312.
- Burghes, A.H. and Beattie, C.E. (2009) Spinal muscular atrophy: why do low levels of survival motor neuron protein make motor neurons sick? *Nat. Rev. Neurosci.*, **10**, 597–609.
- Nicole, S., Diaz, C.C., Frugier, T. and Melki, J. (2002) Spinal muscular atrophy: recent advances and future prospects. *Muscle Nerve*, **26**, 4–13.
- Iascone, D.M., Henderson, C.E. and Lee, J.C. (2015) Spinal muscular atrophy: from tissue specificity to therapeutic strategies. *F1000Prime Rep.*, **7**, 04.
- Nicole, S., Desforges, B., Millet, G., Lesbordes, J., Cifuentes-Diaz, C., Vertes, D., Cao, M.L., De Backer, F., Languille, L., Roblot, N. et al. (2003) Intact satellite cells lead to remarkable protection against Smn gene defect in differentiated skeletal muscle. *J. Cell. Biol.*, **161**, 571–582.
- Frugier, T., Tiziano, F.D., Cifuentes-Diaz, C., Miniou, P., Roblot, N., Dierich, A., Le Meur, M. and Melki, J. (2000) Nuclear targeting defect of SMN lacking the C-terminus in a mouse model of spinal muscular atrophy. *Hum. Mol. Genet.*, **9**, 849–858.
- Gavrilina, T.O., McGovern, V.L., Workman, E., Crawford, T.O., Gogliotti, R.G., DiDonato, C.J., Monani, U.R., Morris, G.E. and Burghes, A.H. (2008) Neuronal SMN expression corrects spinal muscular atrophy in severe SMA mice while muscle-specific SMN expression has no phenotypic effect. *Hum. Mol. Genet.*, **17**, 1063–1075.
- Passini, M.A., Bu, J., Roskelley, E.M., Richards, A.M., Sardi, S.P., O'Riordan, C.R., Klinger, K.W., Shihabuddin, L.S. and Cheng, S.H. (2010) CNS-targeted gene therapy improves survival and motor function in a mouse model of spinal muscular atrophy. *J. Clin. Invest.*, **120**, 1253–1264.
- Rajendra, T.K., Gonsalvez, G.B., Walker, M.P., Shpargel, K.B., Salz, H.K. and Matera, A.G. (2007) A *Drosophila melanogaster* model of spinal muscular atrophy reveals a function for SMN in striated muscle. *J. Cell. Biol.*, **176**, 831–841.
- Chan, Y.B., Miguel-Aliaga, I., Franks, C., Thomas, N., Trulzsch, B., Sattelle, D.B., Davies, K.E. and van den Heuvel, M. (2003) Neuromuscular defects in a *Drosophila* survival motor neuron gene mutant. *Hum. Mol. Genet.*, **12**, 1367–1376.
- Imlach, W.L., Beck, E.S., Choi, B.J., Lotti, F., Pellizzoni, L. and McCabe, B.D. (2012) SMN is required for sensory-motor circuit function in *Drosophila*. *Cell*, **151**, 427–439.
- Lotti, F., Imlach, W.L., Saieva, L., Beck, E.S., Hao le, T., Li, D.K., Jiao, W., Mentis, G.Z., Beattie, C.E., McCabe, B.D. et al. (2012) An SMN-dependent U12 splicing event essential for motor circuit function. *Cell*, **151**, 440–454.
- Timmerman, C. and Sanyal, S. (2012) Behavioral and electrophysiological outcomes of tissue-specific Smn knockdown in *Drosophila melanogaster*. *Brain Res.*, **1489**, 66–80.
- McWhorter, M.L., Monani, U.R., Burghes, A.H. and Beattie, C.E. (2003) Knockdown of the survival motor neuron (Smn) protein in zebrafish causes defects in motor axon outgrowth and pathfinding. *J. Cell. Biol.*, **162**, 919–931.
- Boon, K.L., Xiao, S., McWhorter, M.L., Donn, T., Wolf-Saxon, E., Bohnsack, M.T., Moens, C.B. and Beattie, C.E. (2009) Zebrafish survival motor neuron mutants exhibit presynaptic neuromuscular junction defects. *Hum. Mol. Genet.*, **18**, 3615–3625.
- Hao le, T., Duy, P.Q., Jontes, J.D., Wolman, M., Granato, M. and Beattie, C.E. (2013) Temporal requirement for SMN in motor neuron development. *Hum. Mol. Genet.*, **22**, 2612–2625.
- Giacomotto, J., Rinkwitz, S. and Becker, T.S. (2015) Effective heritable gene knockdown in zebrafish using synthetic microRNAs. *Nat. Commun.*, **6**, 7378.
- Giacomotto, J. and Segalat, L. (2010) High-throughput screening and small animal models, where are we? *Br. J. Pharmacol.*, **160**, 204–216.

20. Giacomotto, J., Segalat, L., Carre-Pierrat, M. and Gieseler, K. (2012) *Caenorhabditis elegans* as a chemical screening tool for the study of neuromuscular disorders. Manual and semi-automated methods. *Methods*, **56**, 103–113.
21. Giacomotto, J., Brouilly, N., Walter, L., Mariol, M.C., Berger, J., Segalat, L., Becker, T.S., Currie, P.D. and Gieseler, K. (2013) Chemical genetics unveils a key role of mitochondrial dynamics, cytochrome c release and IP3R activity in muscular dystrophy. *Hum. Mol. Genet.*, **22**, 4562–4578.
22. Asakawa, K. and Kawakami, K. (2008) Targeted gene expression by the Gal4-UAS system in zebrafish. *Dev. Growth Differ.*, **50**, 391–399.
23. Arkhipova, V., Wendik, B., Devos, N., Ek, O., Peers, B. and Meyer, D. (2012) Characterization and regulation of the hb9/mnx1 beta-cell progenitor specific enhancer in zebrafish. *Dev. Biol.*, **365**, 290–302.
24. Berger, J. and Currie, P.D. (2013) 503unc, a small and muscle-specific zebrafish promoter. *Genesis*, **51**, 443–447.
25. Punnamoottil, B., Rinkwitz, S., Giacomotto, J., Svahn, A.J. and Becker, T.S. (2015) Motor neuron-expressed microRNAs 218 and their enhancers are nested within introns of Slit2/3 genes. *Genesis*, **53**, 321–328.
26. Lewis, K.E. and Eisen, J.S. (2003) From cells to circuits: development of the zebrafish spinal cord. *Prog. Neurobiol.*, **69**, 419–449.
27. Merlini, L., Granata, C., Bonfiglioli, S., Marini, M.L., Cervellati, S. and Savini, R. (1989) Scoliosis in spinal muscular atrophy: natural history and management. *Dev. Med. Child. Neurol.*, **31**, 501–508.
28. Roso, V., Bitu Sde, O., Zanoteli, E., Beteta, J.T., de Castro, R.C. and Fernandes, A.C. (2003) [Surgical treatment of scoliosis in spinal muscular atrophy]. *Arq. Neuropsiquiatr.*, **61**, 631–638.
29. Akitake, C.M., Macurak, M., Halpern, M.E. and Goll, M.G. (2011) Transgenerational analysis of transcriptional silencing in zebrafish. *Dev. Biol.*, **352**, 191–201.
30. Mosimann, C. and Zon, L.I. (2011) Advanced zebrafish transgenesis with Tol2 and application for Cre/lox recombination experiments. *Methods Cell Biol.*, **104**, 173–194.
31. Kwan, K.M., Fujimoto, E., Grabher, C., Mangum, B.D., Hardy, M.E., Campbell, D.S., Parant, J.M., Yost, H.J., Kanki, J.P. and Chien, C.B. (2007) The Tol2kit: a multisite gateway-based construction kit for Tol2 transposon transgenesis constructs. *Dev. Dyn.*, **236**, 3088–3099.
32. Djiotsa, J., Verbruggen, V., Giacomotto, J., Ishibashi, M., Manning, E., Rinkwitz, S., Manfroid, I., Voz, M.L. and Peers, B. (2012) Pax4 is not essential for beta-cell differentiation in zebrafish embryos but modulates alpha-cell generation by repressing arx gene expression. *BMC Dev. Biol.*, **12**, 37.
33. Ishibashi, M., Manning, E., Shoubridge, C., Krecsmarik, M., Hawkins, T.A., Giacomotto, J., Zhao, T., Mueller, T., Bader, P.I., Cheung, S.W. et al. (2015) Copy number variants in patients with intellectual disability affect the regulation of ARX transcription factor gene. *Hum. Genet.*, **134**, 1163–1182.
34. Svahn, A.J., Giacomotto, J., Graeber, M.B., Rinkwitz, S. and Becker, T.S. (2015) miR-124 contributes to the functional maturity of microglia. *Dev. Neurobiol.*, doi: 10.1002/dneu.22328.